








Cite this: *Med. Chem. Commun.*,  
2018, 9, 667

## Crystallomycin revisited after 60 years: aspartocins B and C†

Anton P. Tyurin, <sup>‡,ab</sup> Vera A. Alferova, <sup>‡,a</sup> Alexander S. Paramonov,<sup>‡,b</sup>  
Maxim V. Shuvalov,<sup>ac</sup> Irina A. Malanicheva,<sup>a</sup> Natalia E. Grammatikova,<sup>a</sup>  
Pavel N. Solyev, <sup>d</sup> Shaowei Liu,<sup>e</sup> Chenghang Sun, <sup>e</sup> Igor A. Prokhorenko,<sup>ab</sup>  
Tatyana A. Efimenko,<sup>a</sup> Larisa P. Terekhova,<sup>a</sup> Olga V. Efremenkova,<sup>a</sup>  
Zakhar O. Shenkarev <sup>\*bf</sup> and Vladimir A. Korshun <sup>\*ab</sup>

The study of an archived sample of crystallomycin complex using HPLC, ESI HRMS, and 2D NMR showed that two major components of the antibiotic, compounds **1** and **2**, are lipopeptides having the same peptide core, Asp1-cyclo(Dab2-Pip3-MeAsp4-Asp5-Gly6-Asp7-Gly8-Dab9-Val10-Pro11-), *N*-acylated either with  $\Delta^3$ -iso-tetradecenoyl or  $\Delta^3$ -anteiso-pentadecenoyl that are identical to aspartocins C and B, respectively. According to the 2D NMR study, compound **2** in DMSO solution exists as a mixture of four conformers. The producing strain was identified as *Streptomyces griseorubens*. Compounds **1** and **2** have considerable  $\text{Ca}^{2+}$ -dependent activity against Gram-positive bacteria including five MRSA strains.

Received 2nd January 2018,  
Accepted 25th February 2018

DOI: 10.1039/c8md00002f

rsc.li/medchemcomm

### 1. Introduction

Lipopeptide antibiotics were discovered in the ‘golden era’ of 1950–60s, however, their structure elucidation took several subsequent decades.<sup>1</sup> Crystallomycin was reported by Gause and co-workers in 1957 and named after its ability to crystallize from ethanol.<sup>2</sup> Two years later, a chemical study<sup>3</sup> appeared where a conclusion was made that crystallomycin is very similar, if not identical, to amphomycin,<sup>4</sup> discovered a few years before. However, direct microbiological comparison<sup>5</sup> of crystallomycin and amphomycin showed the same activity spectrum, but incomplete cross-resistance, thus suggesting these two antibiotics are not identical. No further chemical study of crystallomycin was reported. At present, interest in amphomycin-type antibiotics re-emerged, because they are considered to be good precursors in development of novel therapeutic agents against multidrug resistant Gram-positive pathogens.<sup>6</sup> Here we report the study of an archived sample of crystallomycin.

<sup>a</sup> Gause Institute of New Antibiotics, B. Pirogovskaya 11, Moscow 119021, Russia. E-mail: v-korshun@yandex.ru

<sup>b</sup> Shemyakin-Ovchinnikov Institute of Bioorganic Chemistry, Miklukho-Maklaya 16/10, Moscow 117997, Russia. E-mail: zakhar-shenkarev@yandex.ru

<sup>c</sup> Department of Chemistry, Lomonosov Moscow State University, 1-3 Leninskie Gory, Moscow 119992, Russia

<sup>d</sup> Engelhardt Institute of Molecular Biology, Vavilova 32, Moscow 119991, Russia

<sup>e</sup> Institute of Medicinal Biotechnology, Chinese Academy of Medical Sciences & Peking Union Medical College, Tian Tan Xi Li 1, Beijing 100050, China

<sup>f</sup> Moscow Institute of Physics and Technology, Institutsky lane 9, Dolgoprudny, Moscow region 141700, Russia

† Electronic supplementary information (ESI) available. See DOI: 10.1039/c8md00002f

‡ Equal contribution.

### 2. Results and discussion

#### 2.1. Identification and activity studies

The sealed glass ampoule containing a crystallomycin sample isolated 60 years ago was found in the antibiotic collection of the Gause Institute of New Antibiotics (Moscow, Russia). The sample, stored in a refrigerator at 0...+5 °C, is a loose, off-white powder (Fig. 1). Its HPLC analysis indicated a mixture of two major and several minor components (Fig. 2).

Both major compounds were isolated using semi-preparative HPLC; 5.6 mg of **1** and 17.3 mg of **2** (also named Cryst-1 and Cryst-2 in below NMR studies) were obtained. ESI



Fig. 1 The ampoule (above), its label and the antibiotic sample (below); the label says (in Russian): “Crystallomycin 0.4 g 7/1-57”.

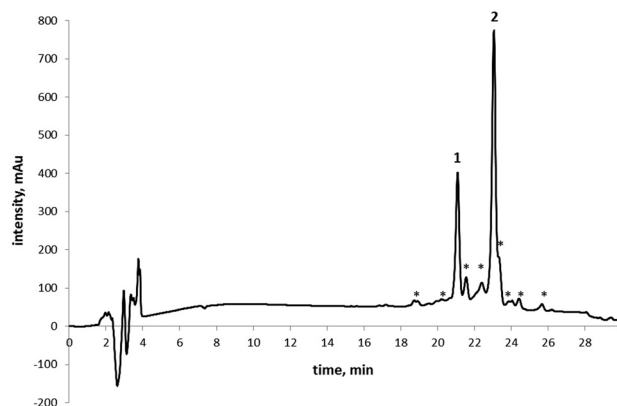


Fig. 2 HPLC profile of crystallomycin complex.

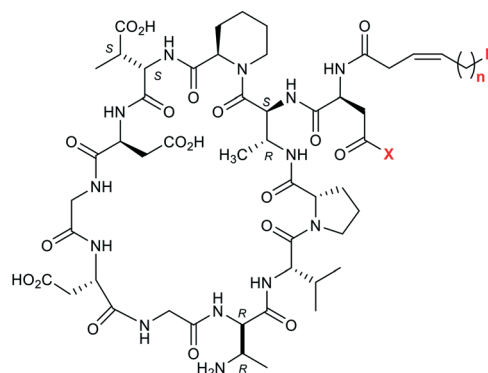
HRMS analysis gave the following  $m/z$  values: 1304.6731,  $[1 + H]^+$ ; 1326.6550,  $[1 + Na]^+$ ; 1348.6373,  $[1 - H + 2Na]^+$ ; 1318.6894,  $[2 + H]^+$ ; 1340.6703,  $[2 + Na]^+$ . The mass of 1 is similar to that reported for aspartocin C, while the mass of 2 is similar to that of aspartocins A and B (within 1 ppm difference). Aspartocins are acidic antibiotics of the amphomycin family (Fig. 3).

The cyclopeptide structure of the two main representatives of this type of antibiotics – friulimicin B and aspartocin C – was correctly described for the first time only in 2000 using 2D NMR techniques.<sup>9</sup> For a long time before the revision, a linear structure with a C-terminal diketopiperazine moiety had been assigned to amphomycin by Bodanszky.<sup>13</sup> For some related compounds, e.g. zaomycin,<sup>14</sup> glumamycin,<sup>15</sup> parvulines,<sup>16</sup> and antibiotic 33,<sup>17</sup> described as similar to amphomycin, the unambiguous structure is still to be determined. Tsushimycin, an antibiotic isolated from culture *S. pseudogriseolus*, contains at least two different types of fatty acid moieties.<sup>18</sup> Nevertheless, authors of the paper<sup>10</sup> referred only to one component as ‘tsushimycin’. To highlight the difference, we use designations A and B in Fig. 3 for these lipopeptides.

Next, crystallomycins 1 and 2 were examined using various 1D and 2D NMR techniques.<sup>19</sup> Sequential  $^1H$  assignment was done using a standard approach based on combination of 2D TOCSY and NOESY spectra.<sup>20</sup> The study revealed the identity of compound 2 to aspartocin B (A-1437 G/tsushimycin B) and of compound 1 to aspartocin C (A-1437 B/tsushimycin A); see section 2.2 below.

Crystallomycin producing strain 00887 was isolated in 1955. It was stored in Gause Institute strain collection (as *Actinomyces violaceoniger* INA 00887). 16S rRNA gene sequence revealed that the strain belongs to genus *Streptomyces* and species *S. griseorubens*. The nucleotide sequence of 16S rRNA gene of the *Streptomyces griseorubens* strain was submitted to NCBI under GeneBank accession number MG200163 and phylogenetic analysis was carried out (Fig. 4).

The HPLC-MS analysis of extract from freshly prepared fermentation broth shows the presence of two peaks fully identical with 1 and 2 from authentic sample (Fig. S6<sup>†</sup>).



Antibiotic	X	n	R	Producing strain	Ref.
Aspartocin A	OH	8	<i>iPr</i>	<i>Streptomyces griseus</i> var. <i>spiralis</i> , <i>S. violaceus</i>	7
Aspartocin B				«-»	7
A-1437 G	OH	7	2-Bu	<i>Actinoplanes friuliensis</i>	8,9
Tsushimycin B				<i>S. pseudogriseolus</i>	10,11
Aspartocin C				<i>S. griseus</i> , <i>S. violaceus</i>	7
A-1437 B	OH	7	<i>iPr</i>	<i>A. friuliensis</i>	8,9
Tsushimycin A				<i>S. pseudogriseolus</i>	10,11
Aspartocin D	OH	5	<i>iPr</i>	<i>S. canus</i>	12
Aspartocin E	OH	4	<i>iPr</i>	«-»	12
Amphomycin				«-»	4,12
A-1437 E	OH	5	2-Bu	<i>A. friuliensis</i>	8,9
A-1437 A	OH	6	<i>iPr</i>	«-»	8,9
Friulimicin A	NH <sub>2</sub>	6	<i>iPr</i>	«-»	8,9
A-1437 C				«-»	8,9
Friulimicin B	NH <sub>2</sub>	7	<i>iPr</i>	«-»	8,9
A-1437 D				«-»	8,9
Friulimicin C	NH <sub>2</sub>	5	2-Bu	«-»	8,9
A-1437 F				«-»	8,9
Friulimicin D	NH <sub>2</sub>	7	2-Bu	«-»	8,9
A-1437 H				«-»	8,9

Fig. 3 Antibiotics of the amphomycin family.

Compounds 1 and 2 show activity towards Gram-positive bacteria, including methicillin- and vancomycin-resistant strains (Table 1), and no activity towards Gram-negative bacteria, yeasts and fungi. Both compounds exhibit strong increase of activity in calcium-adjusted media (2–8-fold decrease in MIC). This is a common feature of calcium-dependent lipopeptides.

## 2.2. NMR studies

The samples of the major compound 2 (‘Cryst-2’) were studied in DMSO- $d_6$ , CD<sub>3</sub>OD, and H<sub>2</sub>O + D<sub>2</sub>O. The  $^{15}N$ -HSQC spectra measured in DMSO- $d_6$  (Fig. 5) revealed the signals of HN-groups, indicating that Cryst-2 has a polypeptide part. However, the observed  $^1H$ - $^{15}N$  cross-peaks demonstrated unequal intensities, and their number significantly exceeded the number of HN-groups expected for the peptide with MW ~1.3 kDa (Fig. 5). Comparison of  $^{15}N$ -HSQC spectra measured at 20, 30, and 45 °C showed that some of these signals became significantly broadened (even beyond the detection limit) at elevated

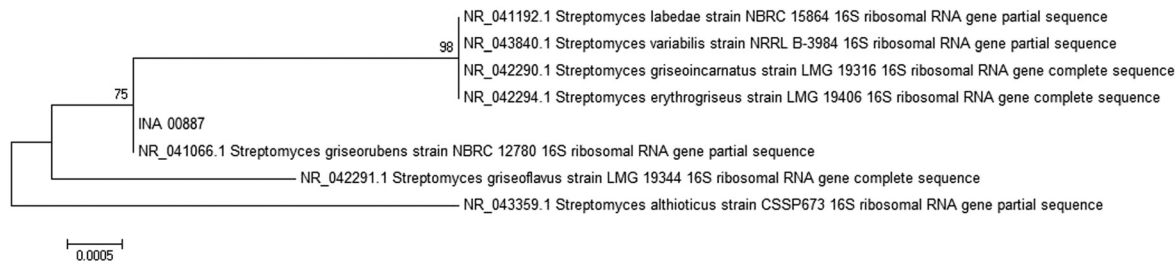


Fig. 4 Phylogenetic tree of strain INA 00887 on the basis of 16S rRNA gene sequence. Scale –5 nucleotide substitutions per 10 000 nucleotides. Bootstrap values (%) were calculated from 100 trees.

temperature (Fig. 5, dotted). The observed signal doubling and broadening arise from the conformational heterogeneity of Cryst-2 molecule in solution (see below). Probably, the corresponding conformational exchange processes take place on ms–s time scale, thus approaching intermediate regime at 45 °C. This induces broadening of some of the resonances. An attempt to shift these exchange processes to the fast regime by increasing the NMR data acquisition temperature was unsuccessful due to considerable degradation of the Cryst-2 compound at 70 °C. Thus, the optimal temperature for NMR study of Cryst-2 was 30 °C (Fig. 5).

Analysis of the 2D TOCSY, COSY, <sup>13</sup>C-HSQC, and 3D TOCSY-<sup>13</sup>C-HSQC spectra revealed the set of the narrow signals corresponding to the fatty acid residue (FA). This FA contains 15 carbon atoms, 14 of which have attached protons (Fig. 6, Table 2). The cross-peak between 2-CH<sub>2</sub>-group of FA and HN-group of Asp1 residue observed in the NOESY spectrum revealed a connection between the peptide and lipid parts of Cryst-2, indicating that the compound is a lipopeptide. The multiplicity edited <sup>13</sup>C-HSQC spectrum allowed to distinguish signals of CH and CH<sub>2</sub> groups. The two CH groups having chemical shifts typical to substituted alkenes (5.47/123.5 and 5.46/132.2 ppm,  $\delta_{\text{H}}/\delta_{\text{C}}$ , respectively) were assigned to the positions 3 and 4 of FA (Fig. 6A, Table 2). Another CH group is located at the position 12 of FA (Fig. 6B), where an attached methyl-group (Me-12) corre-

sponds to the branching in the fatty chain. Two methyl groups of FA (Me-12 and Me-13) having chemical shifts of 0.83/11.7 and 0.82/19.6 ppm ( $\delta_{\text{H}}/\delta_{\text{C}}$ , respectively) display characteristic pattern of overlapped quartet and triplet in the 1D <sup>1</sup>H spectrum (Fig. 6C, inset). Thus, FA moiety in the Cryst-2 lipopeptide has one double bond and two methyl-groups. Such FA residue had previously been identified in the aspartocin B antibiotic.<sup>7</sup> One set of NMR signals was observed for the majority of the FA groups. At the same time, the resonances of 2-CH<sub>2</sub>, 3-CH, and 4-CH groups were split into several parts (see Fig. 6A). Thus, the conformational heterogeneity of Cryst-2 molecule in DMSO solution originates from the exchange processes taking place in the peptide part of the antibiotic.

To investigate the structure of the peptide moiety of Cryst-2, the spin-systems of individual residues were identified in the 2D TOCSY and COSY spectra. The sequential connections were established *via* HN<sub>i-1</sub>-HN<sub>i</sub>, HC<sup>α</sup><sub>i-1</sub>-HN<sub>i</sub> and/or HC<sup>β</sup><sub>i-1</sub>-HN<sub>i</sub> cross-peaks in the NOESY spectra. The observed broadening and splitting of the signals significantly complicated the analysis of <sup>13</sup>C-HMBC spectra. This made it impossible to establish unambiguous sequential connectivities through <sup>13</sup>C resonance frequencies. The obtained NMR data revealed that the peptide part of Cryst-2 is identical to the peptide parts of aspartocin antibiotics and represents the 11-residue peptide cyclized through the β-amino group of 2,3-diaminobutyric acid (Dab2).<sup>7</sup> Thus the major component of Crystalomicin antibiotic coincides with the aspartocin B lipopeptide. The close correspondence observed between <sup>13</sup>C-HSQC spectra of Cryst-2 and aspartocin B<sup>7</sup> in CD<sub>3</sub>OD solution (Fig. S1†) together with the high-resolution mass spectrometry data (*m/z* 1318.6889) confirms the identity of these antibiotics.

Detailed analysis of NMR spectra permitted to identify at least four sets of signals for the majority of residues in the peptide part of Cryst-2 (Table 2). It suggests that the molecule adopts at least four different conformations in solution. These forms denoted as **a**, **b**, **c**, **d** have the relative population of about 100:70:65:30 (Fig. 5B and 6C). The system of intra-conformer cross-peaks observed in the NOESY and ROESY spectra (Fig. 7A and S2 and S3†) indicated that these structural states of Cryst-2 are interconnected by conformational exchange processes. Using intensities of the diagonal and exchange cross-peaks

Table 1 Minimum inhibitory concentrations (MIC) of crystallomycins 1 and 2 against Gram-positive bacteria, μg mL<sup>-1</sup>

Microorganism	Antimicrobial <sup>a</sup>				
	Cub	1(Ca <sup>2+</sup> )	1	2(Ca <sup>2+</sup> )	2
<i>S. aureus</i> ATCC 29213	0.5	4	16	2	4–8
MRSA 86	1	4	16	2	8
MRSA 88	0.5–1	4	16	2	8
MRSA 71001	0.5–1	4	16	2	8
MRSA 20450	1	2	16	1–2	8
MRSA 17	2	4	nd <sup>b</sup>	4	8
<i>S. epidermidis</i> C2001 (MR)	1	4	16	2	4–8
<i>S. epidermidis</i> 004-T1 (MR)	1	4	32	4	16
<i>S. epidermidis</i> 20459 (MR)	1	4	nd	4	nd
<i>E. faecalis</i> ATCC 29212	4	8	nd	8	16
<i>E. gallinarum</i> VP4147	8	4–8	nd	4–8	16

<sup>a</sup> Cub – cubicin (daptomycin); (Ca<sup>2+</sup>) – in the presence of calcium ions (1.25 mM). <sup>b</sup> nd – not determined.

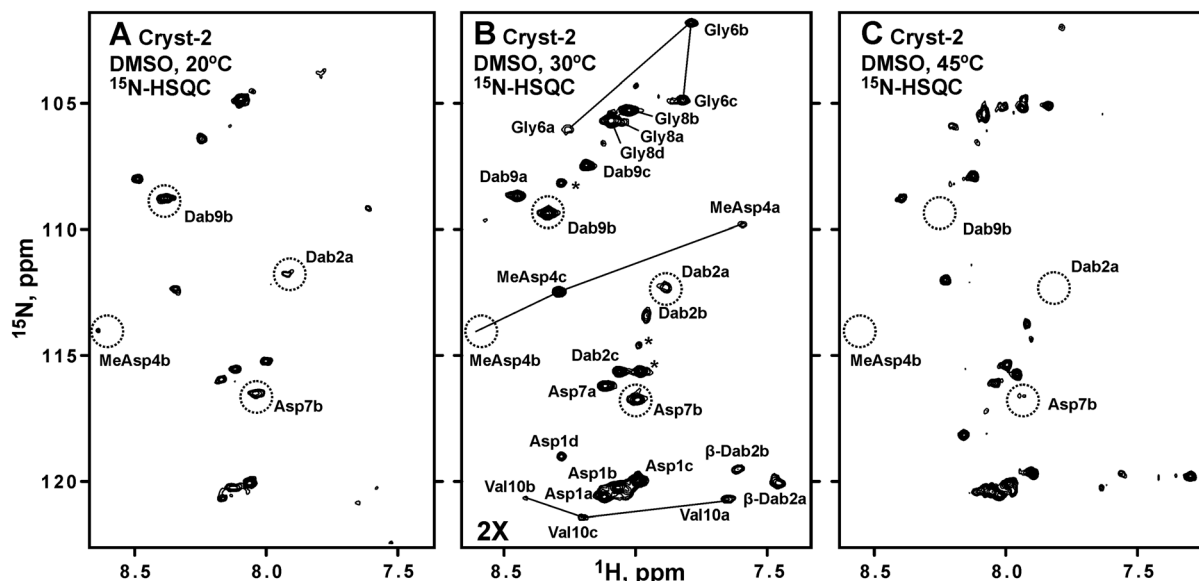


Fig. 5 2D  $^1\text{H}$ ,  $^{15}\text{N}$ -HSQC spectra of Cryst-2 in DMSO- $d_6$  at 20 °C (A), 30 °C (B) and 45 °C (C). The spectra on the panels A and C were measured and processed using identical parameters. The longer measurement time was used for the spectrum on the panel B; and, therefore, this spectrum is drawn with a lower threshold. The obtained resonance assignment of HN-groups is shown on the panel B. Signals of the four different Cryst-2 conformational states are marked using lowercase letters (a, b, c, d). The HN cross-peaks of MeAsp4, Gly6, and Val10 in the a, b, and c conformers are connected by lines. The resonances that became broadened at 45 °C are marked by dotted circles. It should be noted that not all expected HN cross-peaks for the four structural forms of Cryst-2 were identified in the spectra. Some resonances are under the drawing threshold. The unassigned resonances are shown by asterisks. These resonances could belong to the unidentified atoms of the Cryst-2 conformers or originated from impurities in the sample.

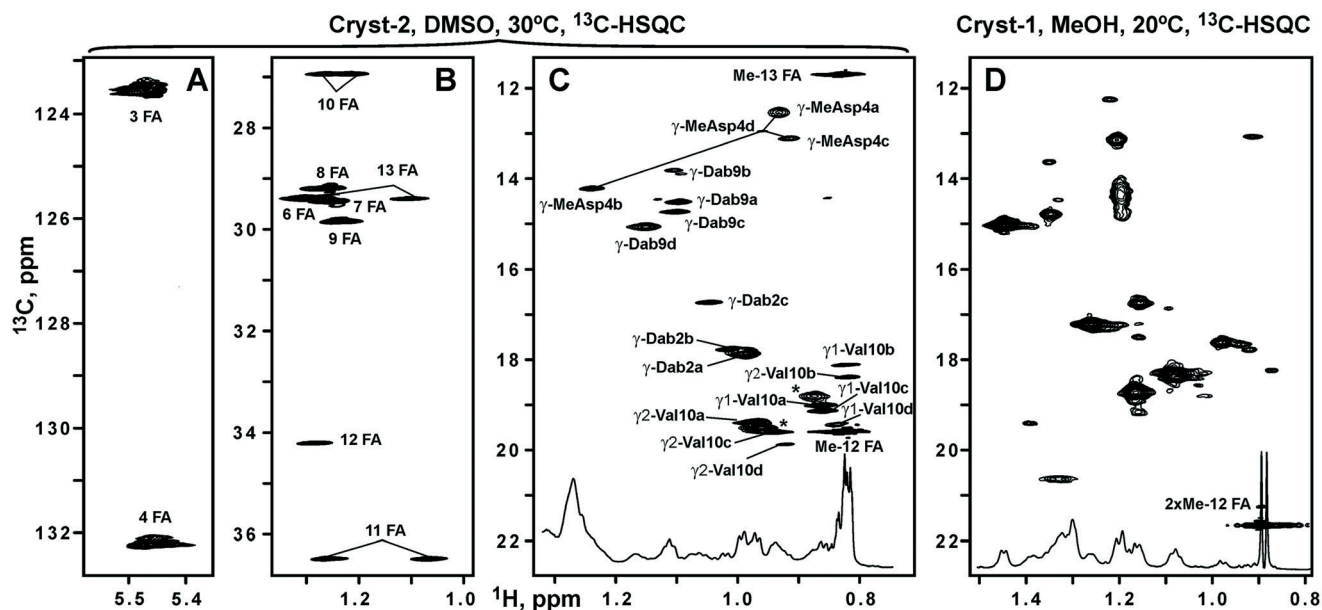


Fig. 6 The fragments of 2D  $^1\text{H}$ ,  $^{13}\text{C}$ -HSQC spectra of Cryst-2 (DMSO- $d_6$ , 30 °C) and Cryst-1 (CD $_3$ OH, 20 °C). The obtained resonance assignment of Cryst-2 is shown. Signals of different Cryst-2 conformational states are marked by lowercase letters (a, b, c, d). (A and B) Assignment of the fatty acid moiety (FA) in Cryst-2. (C) Methyl region of the Cryst-2 spectrum showing terminal signals of FA, and resonances of MeAsp4, Dab9 and Val10 residues. The cross-peaks of MeAsp4 in the different structural forms are connected by lines. The unassigned resonances are shown by asterisks. These resonances could belong to additional structural states of Cryst-2 or to the sample impurities. (D) Methyl region of the Cryst-1 spectrum. The signal of the terminal isopropyl group of FA is shown. The lower insets on the panels C and D show corresponding fragments of the 1D  $^1\text{H}$  spectra.

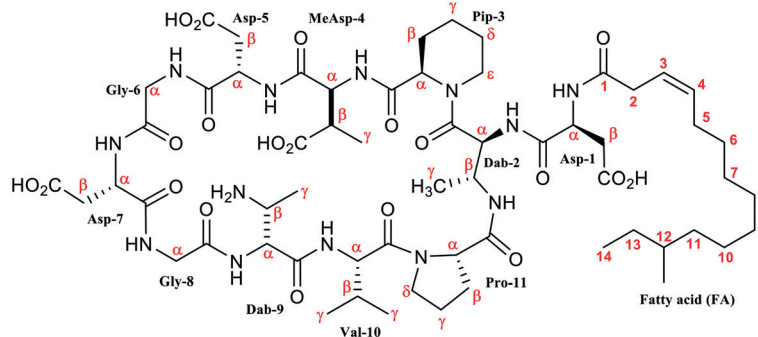
observed for the  $^1\text{H}^\alpha$  proton of Pip3 (Fig. 7A) we estimated the characteristic time of corresponding processes.<sup>19</sup> The exchange processes between conformer a and conformers b, c, and d are going faster (characteristic times  $\sim 1.5$  s) than

exchange  $b \leftrightarrow c$  and  $b \leftrightarrow d$  (characteristic times  $\sim 3$  s). The slowest exchange process was observed between conformers c and d (time  $\sim 8$  s). Therefore the corresponding cross-peaks have lowest amplitude (Fig. 7A).



**Table 2**  $^1\text{H}$ ,  $^{13}\text{C}$  and  $^{15}\text{N}$  chemical shifts (ppm) of the four different conformational states of Cryst-2 lipopeptide (2) in DMSO solution at 30 °C<sup>a</sup>

		Cryst-2 conformer							
		a		b		c		d	
		$\delta_{\text{H}}$	$\delta_{\text{C}}(\delta_{\text{N}})$	$\delta_{\text{H}}$	$\delta_{\text{C}}(\delta_{\text{N}})$	$\delta_{\text{H}}$	$\delta_{\text{C}}(\delta_{\text{N}})$	$\delta_{\text{H}}$	$\delta_{\text{C}}(\delta_{\text{N}})$
Asp1	H <sup>N</sup>	8.12	120.6	8.07	120.2	7.99	120.0	8.28	119.0
	$\alpha$	4.63	50.0	4.68	50.0	4.62	49.8	4.66	50.2
	$\beta$	2.67/2.48	36.8	2.66/2.49	36.9	2.68/2.50	36.5	2.82/2.54	36.4
Dab2	H <sup>N</sup>	7.89	112.3	7.95	113.4	8.06	115.6	8.22	—
	$\alpha$	4.91	53.0	4.92	52.9	4.66	52.4	4.82	53.4
	$\beta$	4.26	46.0	4.26	46.1	4.00	46.5	4.07	46.4
	$\gamma$	0.99	17.8	1.01	17.7	1.05	16.7	1.04	18.2
Pip3	$\beta\text{-H}^{\text{N}}$	7.34	—	7.61	119.5	7.46	120.0	7.47	—
	$\alpha$	4.96	53.6	5.02	53.1	4.79	56.7	5.10	52.8
	$\beta$	2.00/1.68	27.0	2.01/1.51	25.4	2.11/1.55	28.0	2.10/1.99	31.8
	$\gamma$	1.35/1.47	20.5	1.23/1.48	21.0	1.39	20.6	1.54/1.37	20.6
	$\delta$	1.55/1.58	24.6	1.53/1.66	24.7	1.20	24.7	1.60/1.48	24.8
MeAsp4	$\epsilon$	3.80/3.30	43.6	3.03/3.81	44.0	4.26/2.74	40.4	3.93	43.8
	H <sup>N</sup>	7.59	109.9	8.59	114.4	8.29	112.5	7.68	—
	$\alpha$	4.64	54.4	4.12	56.3	4.69	55.0	4.66	54.3
	$\beta$	2.95	40.8	2.76	41.8	2.94	40.9	2.89	41.0
Asp5	$\gamma$	0.93	12.5	1.24	14.2	0.92	13.1	0.97	12.9
	H <sup>N</sup>	8.44	—	—	—	—	—	—	—
	$\alpha$	4.32	51.1	5.00	49.8	5.00	49.7	—	—
Gly6	$\beta$	2.74/2.58	35.5	3.18/2.67	33.3	2.59/3.10	34.0	—	—
	H <sup>N</sup>	8.26	106.0	7.78	101.9	7.82	104.9	—	—
Asp7	$\alpha$	3.68/3.75	42.9	3.60/3.88	41.9	3.90/3.68	42.9	—	—
	H <sup>N</sup>	8.12	116.2	7.98	116.7	—	—	—	—
Gly8	$\alpha$	4.46	50.3	4.66	—	—	—	—	—
	$\beta$	2.59/2.47	36.3	2.74/2.58	36.8	—	—	—	—
	H <sup>N</sup>	8.02	105.2	8.03	105.7	—	—	8.09	105.7
Dab9	$\alpha$	3.80/3.68	42.9	3.88	43.3	3.90/3.64	42.8	3.73/3.87	43.2
	H <sup>N</sup>	8.45	108.6	7.86	107.0	8.19	107.5	8.33	109.4
	$\alpha$	4.71	53.9	4.82	54.0	4.60	53.8	4.72	54.1
Val10	$\beta$	3.61	48.1	3.66	49.5	3.57	48.3	3.58	48.2
	$\gamma$	1.10	14.5	1.11	13.8	1.10	14.7	1.16	15.0
	H <sup>N</sup>	7.65	120.7	8.41	120.5	8.21	121.4	8.14	120.3
	$\alpha$	4.25	56.9	4.38	55.7	4.25	56.9	4.41	56.3
Pro11	$\beta$	2.02	30.2	1.91	32.1	2.06	29.9	2.15	29.5
	$\gamma_1$	0.98	19.4	0.82	18.4	0.94	19.6	0.93	19.8
	$\gamma_2$	0.86	19.0	0.82	18.1	0.86	19.1	0.84	19.4
	$\alpha$	4.15	60.1	4.14	60.0	4.09	60.7	4.47	60.9
	$\beta$	1.70/2.08	30.0	1.70/2.08	29.9	1.79/2.05	29.9	2.09/1.99	32.1
FA	$\gamma$	1.92/1.82	25.1	1.90/1.81	25.1	1.96/1.80	25.0	1.89/1.70	21.8
	$\delta$	3.74/3.55	47.6	3.71/3.49	47.6	3.79/3.57	47.8	3.55/3.32	47.0
	1	—	170.1	—	—	—	—	—	—
	2	2.93	34.4	—	—	—	—	—	—
	3	5.47	123.5	—	—	—	—	—	—
	4	5.46	132.2	—	—	—	—	—	—
	5	1.99	27.4	—	—	—	—	—	—
	6	1.30	29.4	—	—	—	—	—	—
	7	1.26	29.4	—	—	—	—	—	—
	8	1.25	29.2	—	—	—	—	—	—
	9	1.24/1.22	29.8	—	—	—	—	—	—
	10	1.26/1.21	26.9	—	—	—	—	—	—
	11	1.25/1.07	36.5	—	—	—	—	—	—
	12	1.29	34.2	—	—	—	—	—	—
13	1.10/1.28	29.4	—	—	—	—	—	—	
14	0.83	11.7	—	—	—	—	—	—	
Me-12	0.82	19.6	—	—	—	—	—	—	



<sup>a</sup> The four structural forms of Cryst-2 are denoted as a, b, c, d. Inset: structure of Cryst-2 (2).

Due to signal broadening and overlap, some of the resonances from Asp5–Asp7 fragment were not reliably identified in the NMR spectra. For example, the  $^1\text{H}^{\text{N}}$  resonance of Asp5 was observed only for the conformer a in the  $^1\text{H}$  TOCSY and NOESY spectra, but the corresponding HN cross-peak was not

identified in the  $^{15}\text{N}$ -HSQC. Nevertheless, we successfully obtained the  $^1\text{H}$ ,  $^{15}\text{N}$  and  $^{13}\text{C}$  resonance assignment for the four structural forms of Asp1–MeAsp4 and Gly8–Pro11 fragments (Table 2). The connections between these fragments were established *via* NOE contacts between HN <sup>$\gamma$</sup>  of Dab2 and

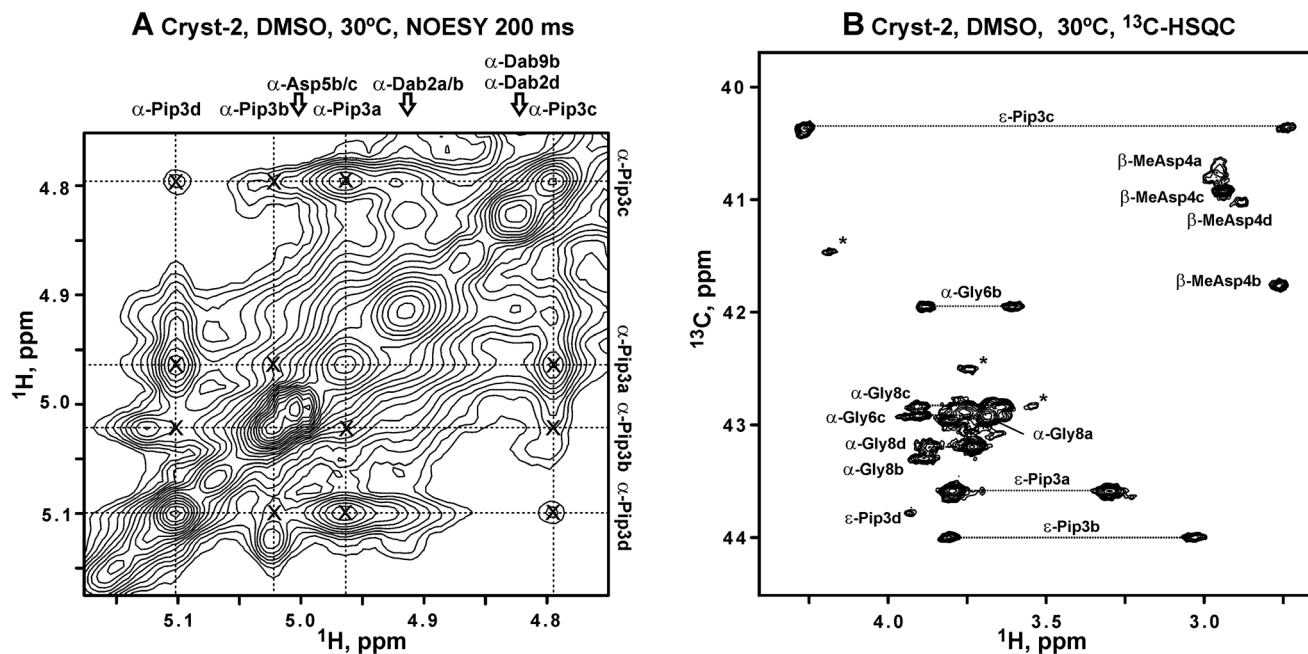


Fig. 7 NMR data reveal exchange processes between the four conformational states of Cryst-2 in DMSO- $d_6$  solution and *cis-trans* isomerization of Dab2–Pip3 peptide bond. (A) The fragment of 2D  $^1\text{H},^1\text{H}$ -NOESY spectrum ( $t_m = 400$  ms). The assignment of  $^1\text{H}^\alpha$  resonances of the Pip3 residue in the a, b, c, and d conformers is shown. The exchange originated (inter-conformer) cross-peaks are marked by crosses. The unassigned resonances probably belong to additional structural states of Cryst-2 or to impurities. (B) Fragment of 2D  $^1\text{H},^{13}\text{C}$ -HSQC spectrum of Cryst-2. Signals of  $\text{CH}_2$  groups are connected by dotted lines. The assignment of  $\text{HC}^\alpha$  resonances of Pip3 residue is shown. Characteristic upfield shift of  $^{13}\text{C}^\epsilon$  resonance in the conformer c confirmed that the corresponding Dab2–Pip3 peptide bond is in the *cis* configuration. According to chemical shift data, the other conformers (a, b, d) of Cryst-2 have *trans* Dab2–Pip3 bonds.

$\text{HC}^{\alpha/\beta}$  of Pro11. The mapping of the assigned fragments to the specific structural forms of Cryst-2 was also supported by the relative cross-peaks intensity in the  $^{13}\text{C}$ -HSQC spectra. Due to significant exchange contribution to the relaxation rates of the nuclei within  $^1\text{H}^{15}\text{N}$ -groups, the comparison of signal intensity in the  $^{15}\text{N}$ -HSQC spectra was found less reliable.

The observed exchange processes could involve *cis-trans* isomerization of the tertiary amide bonds in the peptide part of Cryst-2. The molecule contains two such bonds Dab2–Pip3 and Val10–Pro11. The configuration of Xxx–Pro peptide bonds could be distinguished either using characteristic patterns of NOE cross-peaks ( $\text{HC}^{\alpha_{i-1}}\text{--HC}^{\delta_i}$  for *trans* isomer and  $\text{HC}^{\alpha_{i-1}}\text{--HC}^{\alpha_i}$  for *cis*),<sup>20</sup> or using the difference in the chemical shifts of  $^{13}\text{C}^\beta$  and  $^{13}\text{C}^\gamma$  nuclei of the Pro residue.<sup>21</sup> The corresponding chemical shifts observed in the characteristic regions around 30 and 25 ppm (Table 2), respectively, revealed the *trans* configuration of the Val10–Pro11 bond in the a, b and c conformers ( $\Delta\delta\text{C}^{\beta\gamma} \sim 5.1$  ppm). On the other hand, the  $^{13}\text{C}^\beta$  and  $^{13}\text{C}^\gamma$  chemical shifts of the d conformer (32.1 and 21.8 ppm, respectively,  $\Delta\delta\text{C}^{\beta\gamma}$  of 10.3 ppm) were consistent only with the *cis* configuration.<sup>21</sup> The observation of the strong NOE contacts between  $\text{HC}^\alpha$  of Val10 and  $\text{HC}^\delta$  of Pro11 confirmed *trans* configuration of the Val10–Pro11 bond in the conformers a and c. Crowding in the corresponding spectral region did not permit to use NOE data for analysis of configuration of the b and d conformers.

The same approach could be applied to the determination of the geometry of Xxx–Pip peptide bonds. Indeed, we ob-

served strong NOE contacts between  $\text{HC}^\alpha$  of Dab2 and  $\text{HC}^\epsilon$  of Pip3 in the conformers a, b and d, while the conformer c demonstrated strong NOE between  $\text{HC}^\alpha$  of Dab2 and  $\text{HC}^\alpha$  of Pip3. This indicated that only the conformer c adopts *cis* configuration of the Dab2–Pip3 peptide bond. The comparison of  $^{13}\text{C}$  chemical shifts for Pip3 residue of Cryst-2 with the values reported previously for the *cis*- and *trans*-isomers of pipercolic acid in the ring-opened degradation product of rapamycin<sup>22</sup> also supported this conclusion. The chemical shifts of  $^{13}\text{C}^\alpha$  and  $^{13}\text{C}^\epsilon$  nuclei in the conformers a, b and d were observed in the spectral regions around 53 and 44 ppm, respectively (mean difference 9.4 ppm), while the same atoms in the conformer c resonate at 56.7 and 40.4 ppm (difference 16.3 ppm). These values nicely correspond to the  $^{13}\text{C}^\alpha$  and  $^{13}\text{C}^\epsilon$  chemical shifts observed in the ring-opened rapamycin (50.7 and 43.8 ppm for the *trans*-isomer, and 55.7 and 38.1 ppm for the *cis*-isomer, respectively).<sup>22</sup> Interestingly the conformers c and d, having *cis*-configuration of the different bonds, are connected with the slowest (among observed) exchange process.

The presence of conformational heterogeneity had previously been noted in the NMR study of aspartocin lipopeptides conducted in the DMSO, methanol and acetonitrile/water mixtures,<sup>7,9</sup> but the resonance assignment and structural characterization had been done only for the major isomers of aspartocin A and B. The presently obtained results agree with the previous finding that the configuration of Dab2–Pip3 and Val10–Pro11 bonds is all *trans* in the major structural form of aspartocin B.

The obtained results permit to conclude that the two most populated conformers of the Cryst-2 in DMSO solution (a and b) have identical all-*trans* configuration of the tertiary amide bonds. Thus the difference in their structures could be associated with the more complex structural transition(s), e.g. with the fluctuations in the overall conformation of the cyclic part of the molecule. These fluctuations should be sufficiently slow to provide two distinct sets of NMR resonances and, thus, the a and b states should be separated by the relatively large energetic/enthalpy barrier associated with rupture of several hydrogen bonds or an ionic bond (salt-bridge). Taking into account that the largest changes in the chemical shifts between a and b conformers were observed in MeAsp4–Val10 fragment and especially at MeAsp4 residue (see Fig. 5B and 6C and Table 2), we could propose that one of these conformers is stabilized by ionic interaction between oppositely charged side chain groups of MeAsp4 and Dab9 residues. The other structural forms of the Cryst-2 in DMSO solution also could be stabilized by ionic interactions involving the amino-group of Dab9 and acidic groups of the other residues (e.g. Asp1, Asp5 or Asp7).

The Cryst-2 was also directly solubilized in water (+5% D<sub>2</sub>O). The obtained sample was optically clear, but the 1D <sup>1</sup>H NMR spectra measured at pH in range from 3 to 7 demonstrated very broad lines (Fig. 8). This implies the formation of micelle-like aggregates by the Cryst-2 molecule in water solutions and is consistent with the lipopeptide structure of the compound.<sup>23</sup>

The minor component of the antibiotic, compound 1 (“Cryst-1”) was studied by NMR in CD<sub>3</sub>OH. The 2D <sup>13</sup>C-HSQC spectrum revealed the narrow intense signal of methyl group at 0.89/21.7 ppm ( $\delta_{\text{H}}/\delta_{\text{C}}$ , respectively, Fig. 6D). This signal corresponded to doublet in the 1D <sup>1</sup>H spectrum (Fig. 6D, inset) and therefore belongs to the two overlapped methyl resonances of the isopropyl group. Such FA residues terminating by isopropyl-like moiety (iso-FA) had previously been identified in the aspartocin A and C antibiotics.<sup>7</sup> Taking into account the result of HRMS analysis (*m/z* 1304.6733), we could conclude that the Cryst-1 compound is identical to aspartocin

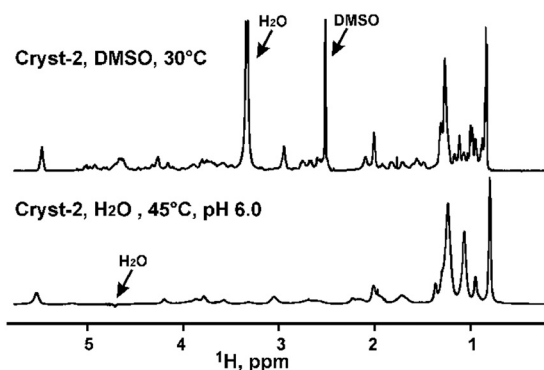


Fig. 8 Comparison of the 1D <sup>1</sup>H spectra of Cryst-2 in DMSO-*d*<sub>6</sub> and in H<sub>2</sub>O (5% D<sub>2</sub>O). The positions of the residual solvent signals are indicated. In the lower spectrum the strong water signal is suppressed by WATERGATE.

C lipopeptide. As compared to aspartocin B (Cryst-2), this antibiotic contains an identical peptide part, but the FA is different ( $\Delta^3$ -iso-14:1 vs.  $\Delta^3$ -anteiso-15:1). The FA residue of aspartocin C is shorter by one CH<sub>2</sub> group and has a different arrangement of two methyl groups. The presence of the additional set of weak signals in the <sup>13</sup>C-HSQC spectrum of Cryst-1 (Fig. 6D) indicated that this lipopeptide also inhere conformational heterogeneity in solution.

The observed conformational heterogeneity significantly complicated NMR analysis of Cryst-1 and -2 lipopeptides. For further structural studies the careful screening of solvent composition is needed to find the experimental conditions where exchange processes are suppressed or slowed down. The membrane mimicking media of detergent micelles or lipid-detergent bicelles could provide such environment.

### 3. Conclusions

In summary, we found that the crystallomycin antibiotic reported in 1957 indeed is similar to compounds of amphomycin lipopeptide family, and contains two major components (identical to aspartocins B and C) along with several minor compounds. The producing strain INA 00887 was cultivated and identified as *Streptomyces griseorubens*. NMR studies of compound 2 (Cryst-2, aspartocin B) in DMSO revealed four major conformers, probably corresponding to the set of (Dab2)–Pip3 and (Val10)–Pro11 rotamers on peptide bonds. Both crystallomycins showed pronounced calcium-dependent activity against Gram-positive bacteria, including several MRSA strains.

### 4. Experimental

#### 4.1. HPLC

Analytical HPLC separations were performed in the following conditions: 20  $\mu$ L of sample (solution of crystallomycin 2 mg mL<sup>-1</sup> in 50% ethanol), column – Waters Sunfire C18 5  $\mu$ m 4.6  $\times$  250 mm, detection at 210 nm, flow rate 1 mL min<sup>-1</sup>, eluent A – 0.1% TFA in water, B – 0.1% TFA in acetonitrile, linear gradient of B, % (time, min): 30(0)  $\rightarrow$  60(25)  $\rightarrow$  75(26)  $\rightarrow$  75(30). Semi-preparative HPLC separations were performed in the following conditions: 200  $\mu$ L of sample (contains 10.9 mg of crystallomycin complex in 50% ethanol), column – Waters XBridge Prep C18 5  $\mu$ m OBD 19  $\times$  150 mm, detection at 210 nm, flow rate 6 mL min<sup>-1</sup>, eluent – 45% acetonitrile/water + 0.1% TFA (isocratic). After analytical re-runs of obtained fractions, the selected fractions with 95+%-content of 1 or 2 were combined. Organic solvent was evaporated under vacuum (bath temp. 30  $^{\circ}$ C), water residue was lyophilized. Compounds 1 (2.0 mg) and 2 (6.8 mg) were obtained as white amorphous powders.

#### 4.2. HRMS

High resolution mass spectra (HRMS) were registered on a Bruker Daltonics microTOF-Q II instrument using electrospray ionization (ESI). The measurements were acquired in a

positive ion mode with the following parameters: interface capillary voltage 4500 V; mass range from  $m/z$  50 to 3000; external calibration (Electrospray Calibrant Solution, Fluka); nebulizer pressure 0.4 bar; flow rate  $3 \mu\text{L min}^{-1}$ ; nitrogen was applied as a dry gas ( $6 \text{ L min}^{-1}$ ); interface temperature was set at  $180 \text{ }^\circ\text{C}$ . Observed  $m/z$  values: 1304.6731 for 1 (calc. 1304.6733 for  $[\text{C}_{59}\text{H}_{93}\text{N}_{13}\text{O}_{20} + \text{H}]^+$ ) (Fig. S4<sup>†</sup>); 1318.6894 for 2 (calc. 1318.6889 for  $[\text{C}_{60}\text{H}_{95}\text{N}_{13}\text{O}_{20} + \text{H}]^+$ ) (Fig. S5<sup>†</sup>).

#### 4.3. Cultivation and extraction

Strain INA 00887 from Gause Institute strain collection was cultivated as described earlier.<sup>2</sup> Fermentation broth (0.25 L) was separated by centrifugation and filtration into culture filtrate and mycelium. The culture filtrate was acidified by aq. HCl to pH = 3.0 and extracted with *n*-butanol ( $2 \times 100 \text{ mL}$ ), the extracts were combined, concentrated *in vacuo* to dryness. The residue was taken up in 1 mL of methanol and then filtered (precipitate discarded). Preliminary antibacterial assay of obtained extract was performed by agar disc ( $d = 6 \text{ mm}$ ) diffusion method as following:  $50 \mu\text{L}$  of the methanol sample was dripped onto each disk, and  $50 \mu\text{L}$  methanol was used as the negative control. The indicator pathogens used for antimicrobial assay were: *Staphylococcus aureus* (ATCC 29213), *Escherichia coli* (ATCC 25922), *Aspergillus niger* (ATCC 16404), *Candida albicans* (ATCC 14053). The inhibition activity was detected only against *S. aureus* strain. The HPLC-MS analysis of obtained extract showed the presence of two peaks fully identical with 1 and 2 from authentic sample (Fig. S6<sup>†</sup>).

#### 4.4. NMR

NMR experiments were carried out on Avance-III-800 and Avance-III-600 spectrometers (Bruker) equipped with 5 mm triple-resonance ( $^1\text{H}$ ,  $^{13}\text{C}$ ,  $^{15}\text{N}$ ) CryoProbes. The Cryst-2 samples contained about 10 mM of the compound in DMSO- $d_6$ , CD<sub>3</sub>OH, or in H<sub>2</sub>O + 5% D<sub>2</sub>O. The Cryst-1 sample contained about 4.5 mM of the compound in CD<sub>3</sub>OH. Spectra were measured in the temperature range from 20 to  $45 \text{ }^\circ\text{C}$ . The following 2D NMR spectra were measured for Cryst-2 in DMSO- $d_6$  using standard gradient-enhanced pulse sequences:<sup>19</sup> DQF-COSY, TOCSY ( $\tau_m = 80 \text{ ms}$ ), NOESY ( $\tau_m = 100, 200, \text{ and } 400 \text{ ms}$ ), ROESY ( $\tau_m = 100 \text{ and } 200 \text{ ms}$ )  $^{15}\text{N}$ -HSQC,  $^{13}\text{C}$ -HSQC, multiplicity edited  $^{13}\text{C}$ -HSQC ( $^{13}\text{C}$ -HSQC-ed),  $^{13}\text{C}$ -HMBC, and 3D TOCSY- $^{13}\text{C}$ -HSQC ( $\tau_m = 80 \text{ ms}$ ). The  $^1\text{H}$  chemical shifts were referenced to the residual CD<sub>2</sub>H signals of CD<sub>3</sub>OH and DMSO- $d_5$  at 3.33 and 2.50 ppm, respectively. Chemical shifts of  $^{13}\text{C}$  and  $^{15}\text{N}$  were referenced indirectly relative to tetramethylsilane (TMS) and liquid NH<sub>3</sub>. To estimate rates of exchange processes, intensities of the diagonal and exchange cross-peaks in NOESY spectrum were fitted to solution of the Bloch-McConnell equations in the Mathematica program (ver. 7, Wolfram Research). The six rates for forward reactions were treated as variables. The backward rates were calculated from equilibrium populations of the states and forward rates assuming microscopic reversibility. R1 relaxation

rates were estimated from 1D inversion recovery experiment ( $\sim 0.55 \text{ s}^{-1}$ ) and assumed to be equal for different states.

#### 4.5. Antibacterial activity

MICs were determined by broth microdilution according to CLSI guidelines<sup>24</sup> with or without Ca<sup>2+</sup> ions. A total of ten clinical isolates such as methicillin-resistant *Staphylococcus* spp. (MRSA and MRSE) and vancomycin-resistant *Enterococcus* spp. were used in this study. *Staphylococcus aureus* ATCC 29213 and *E. faecalis* ATCC 29212 were used as standard microorganisms for quality control of the tests. These strains were obtained from the State collection of pathogenic microorganisms of Tarasevich State Research Institution of Standardization and Control of Biological Medicines. The clinical isolates were obtained from The Russia Research Institute for Antibiotics Culture Collection.

### Conflicts of interest

There authors declare no competing interest.

### Acknowledgements

The research was supported by joint grant from Russian Foundation for Basic Research and National Natural Science Foundation of China (projects 17-53-53130 and 81611530716, respectively). V. A. K. was supported in part by the Molecular and Cellular Biology Program of the Russian Academy of Sciences. P. N. S. was supported in part by the Program of fundamental research for state academies for 2013–2020 years (No. 01201363818). NMR experiments were carried out using equipment provided by the IBCH core facility (CKP IBCH) supported by the Russian Ministry of Education and Science, grant RFMEFI62117X0018. We thank N. G. Machavariani and O. N. Sineva for their helpful advice.

### References

- 1 R. H. Baltz, V. Miao and S. K. Wrigley, *Nat. Prod. Rep.*, 2005, 22, 717–741.
- 2 G. F. Gause, T. P. Preobrazhenskaya, V. K. Kovalenkova, N. P. Il'icheva, M. G. Brazhnikova, N. N. Lomakina, I. N. Kovsharova, V. A. Shorin, I. A. Kunrat and S. P. Shapovalova, *Antibiotiki*, 1957, 2(6), 9–14 (in Russian).
- 3 N. N. Lomakina and M. G. Brazhnikova, *Biokhimiya*, 1959, 24, 425–431 (in Russian).
- 4 B. Heinemann, M. A. Kaplan, R. D. Muir and I. R. Hooper, *Antibiot. Chemother.*, 1953, 3, 1239–1342.
- 5 V. A. Shorin and S. P. Shapovalova, *Antibiotiki*, 1959, 4(1), 77–81 (in Russian).
- 6 (a) C. J. Pasetka, D. J. Erfle, D. R. Cameron, J. J. Clement and E. Rubinchik, *Int. J. Antimicrob. Agents*, 2010, 35, 182–185; (b) W. A. Craig, D. R. Andes and T. Stamstad, *Antimicrob. Agents Chemother.*, 2010, 54, 5092–5098; (c) E. Rubinchik, T. Schneider, M. Elliott, W. R. P. Scott, J. Pan, C. Anklin, H. Yang, D. Dugourd, A. Müller, K. Gries, S. K. Straus, H. G.



- Sahl and R. E. W. Hancock, *Antimicrob. Agents Chemother.*, 2011, 55, 2743–2754; (d) D. Dugourd, H. Yang, M. Elliott, R. Siu, J. J. Clement, S. K. Straus, R. E. W. Hancock and E. Rubinchik, *Antimicrob. Agents Chemother.*, 2011, 55, 3720–3728; (e) M. Singh, J. Chang, L. Coffman and S. J. Kim, *Sci. Rep.*, 2016, 6, 31757.
- 7 F. Kong, K. Janota, J. S. Ashcroft and G. T. Carter, *Rec. Nat. Prod.*, 2010, 4, 131–140.
- 8 W. Aretz, J. Meiwes, G. Seibert, G. Vobis and J. Wink, *J. Antibiot.*, 2000, 53, 807–815.
- 9 L. Vértesy, E. Ehlers, H. Kogler, M. Kurz, J. Meiwes, G. Seibert, M. Vogel and P. Hammann, *J. Antibiot.*, 2000, 53, 816–827.
- 10 G. Bunkóczi, L. Vértesy and G. M. Sheldrick, *Acta Crystallogr., Sect. D: Biol. Crystallogr.*, 2005, 61, 1160–1164.
- 11 (a) J. Shoji, S. Kozuki, S. Okamoto, R. Sakazaki and H. Otsuka, *J. Antibiot.*, 1968, 21, 439–443; (b) H. Nishimura and H. Otsuka, *US Pat.*, 3781420, 1973.
- 12 H. Yang, X. Huang, Z. Zhang, C. Wang, J. Zhou, K. Huang, J. Zhou and W. Zheng, *Nat. Prod. Res.*, 2014, 28, 861–867.
- 13 M. Bodanszky, G. F. Sigler and A. Bodanszky, *J. Am. Chem. Soc.*, 1973, 95, 2352–2357.
- 14 Y. Hinuma, *J. Antibiot., Ser. A*, 1954, 7, 134–136.
- 15 M. Inoue, H. Hitomi, K. Mizuno, M. Fujino, A. Miyake, K. Nakazawa, M. Shibata and T. Kanzaki, *Bull. Chem. Soc. Jpn.*, 1960, 33, 1014–1015.
- 16 E. Toth-Sarudy, I. Horvath, J. Gyimesi, I. Ott, L. Alföldi, J. Berdy, I. Koczka, V. Scholtz, V. Szell and E. Laszlo, *US Pat.*, 3798129, 1974.
- 17 G. F. Gause, T. P. Preobrazhenskaya, I. A. Spiridonova, T. S. Maskimova, O. L. Ol'khovatova, M. G. Brazhnikova, I. V. Tolstykh, V. N. Borisova and G. B. Fedorova, *Antibiotiki*, 1980, 25, 883–887 (in Russian).
- 18 J. Shoji and H. Otsuka, *J. Antibiot.*, 1969, 22, 473–479.
- 19 *Fundamentals of Protein NMR Spectroscopy*, ed. G. S. Rule and T. K. Hitchens, Springer, Dordrecht, 2006.
- 20 K. Wütrich, *NMR of Proteins and Nucleic Acids*, Wiley, New York, 1986.
- 21 M. Schubert, D. Labudde, H. Oschkinat and P. Schmieder, *J. Biomol. NMR*, 2002, 24, 149–154.
- 22 C. C. Zhou, K. D. Stewart and M. K. Dhaon, *Magn. Reson. Chem.*, 2005, 43, 41–46.
- 23 L.-J. Ball, C. M. Goult, J. A. Donarski, J. Micklefield and V. Ramesh, *Org. Biomol. Chem.*, 2004, 2, 1872–1878.
- 24 Clinical and Laboratory Standards Institute (CLSI). Performance standards for antimicrobial susceptibility testing: Twenty fifth informational supplement. CLSI document M100-S25. Wayne, PA: CLSI; 2015. CLSI Methods for dilution antimicrobial susceptibility tests for bacteria that grow aerobically; Approved Standard, 10<sup>th</sup> Ed. CLSI document M07-A10, Wayne, PA, 2015.